Title

Myocardial injection of a thermoresponsive hydrogel with reactive oxygen species scavenger properties improves border zone contractility

Journal

Journal of Biomedical Materials Research Part A, 108(8)

ISSN

1549-3296

Authors

Spaulding, Kimberly A
Zhu, Yang
Takaba, Kiyoaki
et al.

Publication Date

2020-08-01

DOI

10.1002/jbm.a.36941

Peer reviewed

HHS Public Access

Author manuscript

J Biomed Mater Res A. Author manuscript; available in PMC 2021 August 01.

Published in final edited form as:

J Biomed Mater Res A. 2020 August 01; 108(8): 1736–1746. doi:10.1002/jbm.a.36941.

Myocardial injection of a thermoresponsive hydrogel with reactive oxygen species scavenger properties improves border zone contractility

Kimberly A. Spaulding[#a], **Yang Zhu**[#b], **Kiyoaki Takaba**[a], **Anusuya Ramasubramanian**[b], **Anusha Badathala**[a], **Henrik Haraldsson**[a,c], **Alexander Collins**[a], **Esteban Aguayo**[a], **Curran Shah**[b], **Arthur W. Wallace**[a,c], **Nicholas P. Ziats**[d], **David H. Lovett**[a,c], **Anthony J. Baker**[a,c], **Kevin E. Healy**[b,*], **Mark B. Ratcliffe**[a,c,*]

[a]Veterans Affairs Medical Center, San Francisco, CA, 94121, USA

[b]Departments of Bioengineering and Materials Science and Engineering, University of California at Berkeley, CA, 94720, USA

[c]Departments of Anesthesiology, Medicine, Radiology, and Surgery, University of California at San Francisco, CA, 94143, USA

[d]Department of Pathology, Case Western Reserve University, Cleveland, OH, 44106, USA

[#] These authors contributed equally to this work.

Abstract

The decrease in contractility in myocardium adjacent (border zone; BZ) to a myocardial infarction (MI) is correlated with an increase in reactive oxygen species (ROS). We hypothesized that injection of a thermoresponsive hydrogel, with ROS scavenging properties, into the MI would decrease ROS and improve BZ function. Fourteen sheep underwent antero-apical MI. Seven sheep had a comb-like copolymer synthesized from N-isopropyl acrylamide (NIPAAm) and 1500 MW methoxy poly(ethylene glycol) methacrylate, (NIPAAm-PEG1500), injected (20×0.5 mL) into the MI zone 40 minutes after MI (MI+NIPAAm-PEG1500) and seven sheep were MI controls. Cardiac MRI was performed 2 weeks before and 6 weeks after MI+NIPAAm-PEG1500. BZ wall thickness at end systole was significantly higher for MI+NIPAAm-PEG1500 (12.32±0.51 mm/m^2 MI+NIPAAm-PEG1500 vs. 9.88±0.30 MI; p=0.023). Demembranated muscle force development for BZ myocardium 6 weeks after MI was significantly higher for MI+NIPAAm-PEG1500 (67.67±2.61 mN/m^2 MI+NIPAAm-PEG1500 vs. 40.53±1.04 MI; p<0.0001) but not significantly different from remote myocardium or BZ or non-operated controls. Levels of ROS in BZ tissue were significantly lower in the MI+NIPAAm-PEG1500 treatment group (hydroxyl p=0.0031; superoxide p=0.0182). We conclude that infarct injection of the NIPAAm-PEG1500 hydrogel with ROS scavenging properties decreased ROS and improved contractile protein function in the border zone 6 weeks after MI.

[*]Corresponding Authors Mark B. Ratcliffe, MD, Surgical Services (112), Veterans Affairs Medical Center, 4150 Clement Street, San Francisco, California 94121. Telephone: (415) 221-4810. mark.ratcliffe@ucsf.edu; Kevin E. Healy, PhD, 370 Hearst Mining Building, Berkeley, CA 94720. Telephone: (510) 643-3559. kehealy@berkeley.edu.

Keywords

Myocardial Infarction; Myocardial Contraction; Matrix Metalloproteinases-2; Reactive Oxygen Species; Hydrogel

Introduction

Contractile function in the region adjacent (border zone; BZ) to a myocardial infarction (MI) is known to be depressed.[1] While it was initially thought that this reduction in function was secondary to mechanical tethering,[2] mathematical simulations[3] and experimental measurement of contractile protein developed force[4] suggest that there is an intrinsic deficit in adjacent zone contractility. Furthermore, the region involved is larger than previously thought, extending as much as 3 cm from the edge of the MI proper.[5] This decrease in BZ contractile function may contribute to post-MI left ventricular (LV) remodeling and the development of heart failure.

At physiologic levels, reactive oxygen species (ROS) act as secondary signaling messengers in the regulation of myocardial contractility[6,7] by modulation of calcium handling machinery[6] and contractile proteins.[8] ROS contributes to cardiac hypertrophy through action on protein kinases including calmodulin dependent protein kinase II.[6] Nox-2 contributes to post-MI LV remodeling[9] and, at higher ROS, oxidative stress may cause cardiomyocyte apoptosis or necrosis.[10]

There is also substantial evidence that intra-cellular cardiac matrix metalloproteinase (MMP)-2, which exists in two isoforms, mediates the ROS[11,12] effect on myocardial contractility.[13-15] Intracellular full length MMP-2 (FL-MMP-2), normally associated with the sarcomeres in an enzymatically inactive state is activated by ROS with resultant degradation of several key sarcomeric components, including troponin I, myosin light chain-1 and titin.[13-15] Furthermore, ROS stimulates translation of an N-terminal truncated isoform (NTT-MMP-2) that is constitutively active.[11] NTT-MMP-2 is found in greatest abundance within the mitochondrial intramembranous space, where it degrades several key components, including ATP synthetase[11] , and reduces the amplitude of Ca^{2+} transients.[16]

Given the abundant evidence of ROS effect on myocardial contractility and hypertrophy, it is surprising that clinical trials of antioxidants including vitamin E have not shown an effect on cardiac outcomes.[17,18] This raises the question of whether direct myocardial application of ROS scavengers with significantly higher local activity is necessary to achieve an anti-oxidant effect.

Poly(ethylene glycol) (PEG) and PEG-based hydrogels are known ROS scavengers, where ROS cleaves PEG and is consumed in the process.[19,20] To create thermoresponsive polymers, PEG is often copolymerized with with N-isopropyl acrylamide (NIPAAm) as an injectable formulation, which by nature of the PEG monomer would have intrinsic antioxidant properties. For instance, Pollack and Healy described a comb-like copolymer of NIPAAm and PEG methacrylate (mPEGMA) with tunable thermoresponsive characteristics.[21] More recently, Yang *et al.*[22] described a NIPAAm, citric acid, PEG copolymer that was

shown to have intrinsic ROS scavenging properties and minimal inflammatory response in the soft tissue of rats.

In this work, we tested the hypothesis that injection of a thermoresponsive NIPAAm, mPEGMA copolymer hydrogel with ROS scavenging properties would reduce ROS and improve BZ function in a large animal model of myocardial infarction.

Methods

Hydrogel fabrication and characterization.

Materials.—All materials were purchased from Sigma-Aldrich (St. Louis, MO) unless otherwise stated.

Copolymer Synthesis and Formulation.—The synthesis of comb-like NIPAAm, mPEGMA copolymer followed previously published methods.[21] Briefly, 542 mg of N-isopropyl acrylamide (NIPAAm) and 300 mg of 1500 Da methoxy poly(ethylene glycol) methacrylate (mPEGMA) were dissolved in 40 mL of PBS (w/o Ca or Mg) at 2.13 wt% (0.125 mol/L) total monomer concentration. The solution was bubbled with nitrogen for 30 minutes in a septum-capped conical flask and then cooled to 4°C. Next, 38.1 μL of N,N,N',N'-tetramethylethylenediamine (TEMED) (Polysciences, Inc.) was added (10.5 mmol/L) as a catalyst and 57.6 μL of 100 mg/mL ammonium persulfate (APS)/DI water solution was added (0.63 mmol/L) as an initiator under stirring. The solution was sterile-filtered (0.2 μm) and allowed to polymerize under nitrogen and in the dark for 18 hours on ice. The resultant copolymer was 67.3% mole fraction of NIPAAm and 22.7% mole fraction of PEG. At the end of this and the following steps, the product was purified via membrane dialysis (100,000 MW) (Figure 1A).

To conjugate biotin to the NIPAAm-PEG1500, 0.03 mM acrylic acid was copolymerized with NIPAAm and mPEGMA. Subsequently, biotin was grafted by reaction of carboxylic groups with the amine group on amine-PEG11-biotin in the presence of 1-ethyl-3-(3-dimethylaminopropyl) carbodiimide hydrochloride (EDC) in 0.1M (2-N-morpholino) ethanesulfonic acid (MES buffer, pH 4.7) for 4 hours at room temperature.

Hydrogel Degradation.—NIPAAm-PEG1500 was dissolved in ATSM reagent grade I water (18.2 MΩ·cm), and 30% (9.79 M) H_2O_2 (Fisher Scientific, Hampton, NH) was added to the hydrogel solution to make the final hydrogel concentration of 2.5wt% and H_2O_2 concentration at 5% (1.63 M). The dialyzed solution was lyophilized to obtain the H_2O_2 treated polymer before reconstitution for further use.

Hydrogel characterization.—Pristine and H_2O_2 treated NIPAAm-PEG1500 were dissolved in D_2O and ^1H NMR spectra were recorded with a 400 MHz Bruker spectrometer. Hydrogel viscosity during temperature induced sol-gel transition was measured on an Anton Paar rheometer (MCR302). A temperature sweep from 25 to 50°C was performed at a heating rate of 1°C/min, the shear storage modulus G' and the loss modulus G" of the polymer solutions (2.0 wt% in PBS) were collected as a function of temperature at a fixed strain of 1% and a frequency of 1 Hz.

***In vitro* ROS scavenging.—**The Fenton reaction was used to determine hydroxyl radical scavenging and superoxide radical scavenging was determined with a pyrogallol assay as previously described.[23]

Large animal studies.—Sheep (Dorsett cross breed, castrated males) were treated as previously described[24] under a protocol approved by the San Francisco VA Institutional Animal Care and Use Committee (IACUC), in compliance with the "Guide for the Care and Use of Laboratory Animals" prepared by the Institute of Laboratory Animal Resources, National Research Council.

Myocardial infarction.—Fourteen adult sheep underwent antero-apical MI as previously described and the MI controls have been previously reported.[24]

Hydrogel administration.—Six sheep received direct injection of NIPAAm-PEG1500 hydrogel. Injections of 0.5 mL, with 20-25 injection sites 1 cm apart per animal were performed 40 minutes after MI. A representative injection pattern is shown in Figure 2A.

***Ex vivo* Diffusion Tensor Imaging (DTI).—**DTI studies were conducted at the University of Utah Small Animal Imaging Facility on a Bruker Biospec 70/30 instrument (Bruker Biospin, Ettlingen, Germany) using a 3D spin-echo sequence similar to previous studies.[25] The diffusion tensor and fractional anisotropy (FA) were calculated on a voxel by voxel basis. Figure 2B shows the overlay of a 2D short-axis and 2D long-axis slice of the FA maps. FA transition from hydrogel depots to adjacent BZ tissue was analyzed along two perpendicular lines in longitudinal and radial directions through the centers of the hydrogel depots. Results of six depots were pooled for analysis of the trend of FA change outwards from depots.

Cardiac Magnetic Resonance Imaging (CMRI).—CMRI was performed on a 3T MRI scanner (Skyra, Seimens, Malvern, PA) 2 weeks before, and then 2 and 6 weeks after MI as described.[24] Briefly, anesthesia was induced with ketamine (20 mg/kg intravenous) and maintained with isoflurane (2.2% inhaled). Six cine long axis images 30° apart were obtained. Ferumoxytol (0.125 ml/kg IV over 1 hour; AMAG Pharmaceuticals, Waltham, MA) was given prior to CMRI.[26]

Swan Ganz catheter.—Following CMRI, Cardiac output and pulmonary artery wedge pressure (PCWP) measurements were obtained using a Swan Ganz catheter as previously described.[24]

Post-mortem examination.—Sheep were sacrificed six weeks after MI and tissue samples were taken from the MI, BZ, and remote anterior wall for histology, muscle strip mechanics and biochemistry as previously described.[24]

CMRI image analysis.—LV endocardial and epicardial borders were manually contoured (MeVisLab, MeVis Medical Solutions, Bremen, Germany) and 3D cavity and wall volumes of the LV at end-diastole (ED) and end-systole (ES) were calculated (MeVisLab).[24] LV volume measurements were indexed to body surface area[27] to the 1.5 power.[28] LV and MI

segmentation and mesh-based wall thickness and MI area calculations were performed as previously described.[24] Wall thickness was measured at centimeter increments along the LV BZ and each measurement was repeated at each of the 24 elements around the circumference.

Histology and Immunohistochemistry.—Separate samples of tissue from the anterior BZ and remote myocardium were fixed by paraffin-embedded and snap-frozen methods as previously described.[24] Paraffin-embedded sections (5 μm) were stained with hematoxylin and eosin. Snap-frozen tissue was sectioned and stained with Oil red O.

Immunohistochemistry was performed using paraffin-embedded sections as previously described.[24] Primary antibodies used included rabbit antibody to CD31 (Abcam, #28364, dilution 1/50). Omission of primary antibody was used as a negative control. For direct visualization of the biotin-tagged hydrogel, rehydrated tissue sections were incubated with avidin-HRP (Invitrogen A2664 dilution 1/100) for 1 hour at room temperature. Sections stained with anti-CD31 and HRP were counterstained with hematoxylin. Samples were viewed with a Zeiss microscope (Carl Zeiss, Oberkochen, Germany) and images were digitized with an Axiophot camera (Zeiss).

MMP-2 immunohistochemistry.—Immunohistochemistry of FL-MMP-2 and analysis was performed as previously described.[29]

Fluorescent imaging of reactive oxygen species (ROS).—Fluorescent imaging of the anterior BZ and remote myocardium was performed as previously described.[30] Samples were viewed with a Zeiss confocal microscope (LSM 510 Meta Confocal Microscope, Zeiss). Images of ROS stained sections were analyzed using ImageJ (NIH, Bethesda, MD). Specifically, the respective ROS stain was the percent area that was positive with a green filter.

***Ex-vivo* myofilament contractility.—**Epicardial muscle fibers from BZ and remote myocardium were pinned on silicone substrate at physiological sarcomere length and chemically demembranated. Developed force of demembranated myocardial samples was measured as previously described.[4]

Statistical analysis.—All values are expressed as mean±standard error of the mean. A multivariate mixed effect analysis (Proc Mixed, SAS version 9.2, SAS Institute Inc., Cary, NC) was performed. Individual sheep were included as a random effect.[31] The Bonferroni method was used to correct for multiple comparisons. The significance level was set at $p<0.05$.

Results

Structure and properties of NIPAAm-PEG1500 changes after H_2O_2 exposure.

Thermally responsive NIPAAm-PEG1500 was synthesized by radical addition polymerization, and its structure was confirmed with NMR (Figure 1A, D). The molar ratio of NIPAAm and PEG in the copolymer was 2.06:1, as determined from the peak areas on the

NMR spectrum. The concentration of PEG component in the copolymer solution was 0.82 wt%. Since 3:1 was the ratio between NIPAAm and PEG monomers, it shows that the reactivity of NIPAAm was lower compared to PEG1500 in the reaction system.The NIPAAm-PEG1500 solution gelled at 35°C (Figure 1B), lower than the body temperature of adult sheep.[32] The viscosity of NIPAAm-PEG1500 hydrogel was low at room temperature, and as the temperature increased past the lower critical solution temperature (LCST) the modulus increased (Figure 1B). The storage modulus G' was ~3 Pa at sheep body temperature. Rapid gelation of the NIPAAm-PEG1500 solution was demonstrated by direct injection into 37°C water (Figure 1C).

After H_2O_2 treatment, the -CH_2- protons on PEG repeating units (peak A on NMR spectrum) and -CH_2- protons on NIPAAm repeating units (peak C) decrease from 2.5 to 1.72 (Figure 1D), showing the cleavage of PEG side chains. While the viscosity dropped due to H_2O_2 treatment, the LCST of NIPAAm-PEG1500 did not change significantly, as shown in Figure 1B.

ROS scavenging capability of NIPAAm-PEG1500.

The NIPAAm-PEG1500 exhibited ROS scavenging capability *in vitro*. With the Fenton reaction, where hydroxyl radicals are generated predominantly, 2.5 wt% NIPAAm-PEG1500 was capable of scavenging 36% of hydroxyl radicals at the given conditions, significantly higher than blank controls (Figure 1E). A similar effect was observed in superoxide radical generating pyrogallol assay: 38% of the radicals were consumed by NIPAAm-PEG1500 (Figure 1F).

Large animal studies.

Average initial animal weights (MI: and MI+ NIPAAm-PEG1500: kg) and weight gain (MI: and MI+ NIPAAm-PEG1500: kg) in the two groups were similar (SI Table 1).

Hydrogel migration.

Figures 2B and C show the pattern of distribution of NIPAAm-PEG1500 hydrogel immediately after injection. Figure 2B shows the fractional anisotropy (FA) map in XY and YZ planes slicing through a representative hydrogel depot obtained from diffusion tensor CMRI. A clearer gray value view of the same hydrogel depot is given in Figure 2C, as the isotropic hydrogel appeared dark. The area of the hydrogel depots was 1.42±0.16 cm^2 with a volume of 0.57±0.10 mL assuming the depots were elliptical. FA along two perpendicular lines in longitudinal and radial directions through the centers of the hydrogel depot in Figure 2C was depicted in Figure 2D. From the low FA "valley" regions corresponding to the hydrogel, FA increased through the interface of hydrogel and anisotropic BZ myocardium, and reached a plateau deep into the myocardium, indicating hydrogel diffusion into the surrounding tissue upon injection. The trend is clear in Figure 2E, where data from six depots were combined.

Effect on regional LV function.

Representative three chamber long axis CMRI images obtained at end-systole (ES) from control and NIPAAm-PEG1500 hydrogel sheep 6 weeks after MI are seen in Figures 3A and

C respectively. Figures 3B and D are color maps of LV wall thickness at ES in MI control and NIPAAm-PEG1500 hydrogel 6 weeks after MI. Figure 3E shows the effect of NIPAAm-PEG1500 hydrogel LV wall thickness index at ES 6 weeks after MI as a function of distance from the MI. The wall thickness of the MI and remote myocardium at ES was significantly greater in hydrogel treated hearts compared to control (p=0.0426, 0.0226 and 0.0149 at 1, 2 and 3 cm from the MI border).

Effect on global LV function and shape.

Appendix Table 1 shows measurements obtained from CMRI as well as Swan Ganz catheter measurements, including stroke volume and PCWP. Briefly, heart rate, cardiac index, pulmonary capillary wedge pressure, LV cavity volume, stroke volume and ejection fraction in the MI control and NIPAAm-PEG1500 hydrogel groups were not statistically different. The MI area was 3.53+0.43 cm^2 in MI control and 4.20+0.34 cm^2in the NIPAAm-PEG1500 group (19% increase, p=NS).

Histology and immunohistochemistry.

Figure 4 shows histology of BZ tissue 6 weeks after MI±NIPAAm-PEG1500 hydrogel injection. The NIPAAm-PEG1500 hydrogel was broken into small septated portions (Figure 4A) with area of 1,073±45 μm^2 and volume of 29,925±2,100 μm^3 assuming the deposit was a sphere and as outlined by avidin (biotin) positive staining (Figure 4E). Hemorrhage in the hydrogel space was a persistent finding (Figure 4C) and CD31 staining of the hydrogel septate suggests the presence of immature blood vessel formation (Figure 4D). The tissue response was further characterized by minimal foreign body reaction, and fibrosis appeared unchanged from control. Last, there was evidence of migration of the hydrogel into the BZ along planes between myofibers (Figure 4B).

ROS.

Figure 5 shows the effect of NIPAAm-PEG1500 hydrogel on superoxide and hydroxide production in the anterior BZ 6 weeks after MI. Hydroxyl radical was increased by over 3,800% in the BZ 6 weeks after MI when compared with non-operated control, but then decreased by 88% (p=0.0014) in the BZ of NIPAAm-PEG1500 hydrogel treated hearts. Similarly, superoxide was increased by over 6,500% in the BZ 6 weeks after MI when compared with non-operated control, but then decreased by 88% (p=0.0134) in the BZ of NIPAAm-PEG1500 hydrogel treated hearts.

Intracellular MMP-2.

Figure 6A shows immunohistochemical staining for the FL-MMP-2 in the infarct BZ 6 weeks following MI±NIPAAm-PEG1500 hydrogel. Qualitatively, FL-MMP-2 can be observed (purple) in the BZ and remote areas of MI hearts. FL-MMP-2 evenly distributed in all cells in the BZ of MI hearts, while some cells had more FL-MMP-2 compared to adjacent cells in the remote areas. In contrast, staining in non-op control and NIPAAm-PEG1500 hydrogel treated hearts was light universally across the BZ and remote areas. Quantitative analysis showed that FL-MMP-2 expression was 55.7% (p=0.148) higher in MI BZ

compared to MI remote myocardium but then decreased by 62.0% (p=0.0001) in the BZ of NIPAAm-PEG1500 hydrogel treated hearts (Figure 6B).

Ex-vivo myofilament contractility.

Figure 7 shows the effect of NIPAAm-PEG1500 hydrogel on maximum myofilament developed force assessed using demembranated cardiac muscle preparations from the infarct BZ 6 weeks after MI. Developed force was reduced to 48.9% in the BZ 6 weeks after MI when compared with non-operated control and was higher in the BZ of NIPAAm-PEG1500 hydrogel treated hearts (78.17%; p<0.0001).

Discussion

The principal finding of the study was that myocardial injection of a thermoresponsive NIPAAm-PEG1500 hydrogel, with ROS scavenger properties, significantly decreased ROS, increased wall thickness, and improved contractile protein function in the adjacent BZ region six weeks after MI.

Hydrogel migration.

Diffusion tensor (DTI) CMRI images captured immediately after hydrogel injection showed that the hydrogel depots are initially discrete with hydrogel depot volumes consistent with the volume of injections (0.5 mL each). On the other hand, it is necessary for the hydrogel to move into the BZ so that contact between PEG side chains and ROS can occur and ROS can be scavenged *in vivo*. In that regard, there was a gradient in DTI based fractional anisotropy (Figure 2C) extending from the edge of the hydrogel depots into the MI and BZ myocardium which suggests acute migration of hydrogel. This finding is corroborated by histology of the BZ performed 6 weeks after MI and hydrogel injection that shows numerous small septated packets (Figure 4A) some of which were arranged along planes between myofibers (Figure 4B). Taken together, this data suggests that although most of the hydrogel remained in injection site depots, the low modulus hydrogel also moves immediately into MI and BZ regions beyond the injection depots.

Material properties of the NIPAAm-PEG1500 hydrogel likely contribute to gel distribution after injection. For instance, the volume of hydrogel that remains in injection site depots is likely the result of fast phase transition and high molecular weight (10 M g/mol). On the other hand, the low modulus of the baseline hydrogel likely contributes to acute hydrogel migration although Ifkovits *et al.*[33] who injected a significantly stiffer (G'=40 kPa) hyaluronic acid hydrogel immediately following MI noted excellent tissue integration also. Furthermore, the decrease in viscosity associated with cleavage of PEG side chains by ROS may accelerate chronic phase hydrogel migration.

Biological Performance.

The tissue response to the NIPAAm-PEG1500 hydrogel was characterized by both minimal foreign body reaction and fibrosis. The minimal foreign body response may be a result of tissue integration with hydrogel. In other studies that involved injection of synthetic thermally responsive hydrogels, macrophages encapsulated hydrogel when depots were

formed, while less macrophage recruitment was observed when hydrogel had better tissue integration, e.g. penetrated the tissue upon injection or after hydrogel depots were degraded.[23,34] The mechanism of hydrogel septation is unclear, but it is interesting that the gel packet septa were CD31 positive (Figure 4D) and suggesting nascent angiogenesis or vasculogenesis.

ROS scavenging effect.

Our data shows that PEG side chains are able to consume hydroxyl and superoxide radicals in alignment with the mechanism proposed by Ulbricht *et al.*[20] The reduction in the BZ ROS in the animals that received hydrogel injections suggests that the NIPAAm-PEG1500 hydrogel was acutely transported into MI and BZ regions where it successfully scavenged BZ ROS generated by mechanotransduction[9] and inflammatory pathways.[35]

Beneficial effects of NIPAAm-PEG1500 hydrogel on BZ dysfunction.

Consistent with our previous study,[4] we found that force development of myocardium from the infarct BZ was decreased by 34% compared to force development of remote myocardium. Results are also consistent with our previous study of the MMP inhibitor and ROS scavenger,[36] Doxycycline, in which we found increased MLC-1 phosphorylation, increased cross-bridge formation, increased contractile protein developed force *in vitro*,[4] normalized MMP-2 levels and increased wall thickness at end-systole in the BZ six weeks after MI.[24] These findings are consistent with the hypothesis that MMP-2 mediated myofilament damage can be decreased by therapies that decrease ROS upstream of MMP-2.

Infarct expansion.

Although BZ contractility improved, overall LV function in the NIPAAm-PEG1500 group was not different than the control MI group. We suggest that this inconsistency is explained by differences in the infarct area in the two groups where, although not significant, the MI area was 19% higher in the NIPAAm-PEG1500 hydrogel group. Specifically, the stiffness of the NIPAAm-PEG1500 hydrogel (G' ~ 10 Pa) may not have been sufficient to mechanically stabilize the MI area and prevent subsequent infarct expansion. Our observations are consistent with studies by Rane *et al.*,[37] who injected a non-degradable crosslinked PEG hydrogel with G' ~ 500 Pa, into the MI region of rats, and although the MI wall was thicker, LV remodeling was not different.[37] Furthermore, Morita *et al.* [38] injected Radiesse dermal filler with G' ~ 1.4 kPa [39] into the antero-apical MI region of sheep and found that MI area was reduced by 10% 8 weeks later. Finally, Ifkovits *et al.*[40] injected hyaluronic acid hydrogels of low (G'=8 kPa) and high (G'=42 kPa) stiffness immediately following MI. Injection of the low stiffness gel was associated with an MI area reduction of 25% while the high stiffness gel caused the MI area to decrease by 50%. Taken together, these studies suggest that injectate stiffness of ~ 1 kPa is necessary for mechanical stabilization of the MI region. Gels with stiffness < 1 kPa will likely be associated with un-restrained infarct expansion while injection of higher stiffness gels will be associated with infarct contraction.

Future directions.

There is a need for improved hydrogel tracking methods.[33,40] In addition, if optimal results are to be obtained, low modulus hydrogel treatments of the MI BZ need to be coupled with high stiffness gel therapy delivery to the MI proper so as to limit MI expansion and improve LV remodeling.

Limitations.

The main limitation of the current study is our inability to precisely determine spatial distribution of hydrogel *in vivo*. The biotin label that we used was only partially effective, since the hydrogel returns to liquid phase during tissue processing and is lost if it is not infiltrated with tissue. DTI-based fractional anisotropy (FA) is effective in determining the distribution of isotropic hydrogel within the excised heart. Non-invasive imaging methods able to track *in vivo* hydrogel distribution will need to be developed in the future.

Although our focus in the current study was on ROS mediated contractile protein damage, we cannot rule out other mechanisms of hydrogel action. Other causes of BZ dysfunction have been identified including alterations in calcium handling[41], and reduction in high-energy phosphate related energy stores.[42] Further studies are warranted to understand calcium handling and/or energy store related dysfunction of the adjacent zone as a mechanism of hydrogel action.

Conclusions

The principal finding of the study is that direct infarct injection of the thermoresponsive NIPAAm-PEG1500 hydrogel improves contractile protein function, increases wall thickness, and decreases ROS in the BZ 6 weeks after MI. The effect is likely mediated by a reduction in intracellular MMP-2 activity by upstream reduction of ROS. Future improvements in cardiac output may require employing hydrogels with higher moduli that still retain the ability to be injected and migrate to the MI to quench ROS/MMP-2 activity.

Supplementary Material

Refer to Web version on PubMed Central for supplementary material.

Acknowledgement

The authors thank the funding support by National Heart, Lung and Blood Institute Grant R01-HL-084431, Department of Veterans Affairs Merit Review Award I01BX000740, and the American Heart Association: Grant in Aid 14GRNT20380813, and Grant in Aid 15GRNT25550041.

References

1. Jackson BM, Gorman JH, Moainie SL, Guy TS, Narula N, Narula J, John-Sutton MG, Edmunds LH Jr., Gorman RC. Extension of borderzone myocardium in postinfarction dilated cardiomyopathy. J Am Coll Cardiol 2002;40(6):1160–7; discussion 1168-71. [PubMed: 12354444]
2. Homans DC, Asinger R, Elsperger KJ, Erlien D, Sublett E, Mikell F, Bache RJ. Regional function and perfusion at the lateral border of ischemic myocardium. Circulation 1985;71(5):1038–47. [PubMed: 3986974]

3. Guccione JM, Moonly SM, Moustakidis P, Costa KD, Moulton MJ, Ratcliffe MB, Pasque MK. Mechanism underlying mechanical dysfunction in the border zone of left ventricular aneurysm: a finite element model study. Ann Thorac Surg 2001;71(2):654–62. [PubMed: 11235723]
4. Shimkunas R, Makwana O, Spaulding K, Bazargan M, Khazalpour M, Takaba K, Soleimani M, Myagmar BE, Lovett DH, Simpson PC and others. Myofilament dysfunction contributes to impaired myocardial contraction in the infarct border zone. Am J Physiol Heart Circ Physiol 2014.
5. Lee LC, Wenk JF, Klepach D, Zhang Z, Saloner D, Wallace AW, Ge L, Ratcliffe MB, Guccione JM. A novel method for quantifying in-vivo regional left ventricular myocardial contractility in the border zone of a myocardial infarction. J Biomech Eng 2011;133(9):094506. [PubMed: 22010752]
6. Kohler AC, Sag CM, Maier LS. Reactive oxygen species and excitation-contraction coupling in the context of cardiac pathology. J Mol Cell Cardiol 2014;73:92–102. [PubMed: 24631768]
7. Prosser BL, Ward CW, Lederer WJ. X-ROS signaling: rapid mechano-chemo transduction in heart. Science 2011;333(6048):1440–5. [PubMed: 21903813]
8. Sumandea MP, Steinberg SF. Redox signaling and cardiac sarcomeres. J Biol Chem 2011;286(12):9921–7. [PubMed: 21257753]
9. Looi YH, Grieve DJ, Siva A, Walker SJ, Anilkumar N, Cave AC, Marber M, Monaghan MJ, Shah AM. Involvement of Nox2 NADPH oxidase in adverse cardiac remodeling after myocardial infarction. Hypertension 2008;51(2):319–25. [PubMed: 18180403]
10. Seddon M, Looi YH, Shah AM. Oxidative stress and redox signalling in cardiac hypertrophy and heart failure. Heart 2007;93(8):903–7. [PubMed: 16670100]
11. Lovett DH, Mahimkar R, Raffai RL, Cape L, Maklashina E, Cecchini G, Karliner JS. A novel intracellular isoform of matrix metalloproteinase-2 induced by oxidative stress activates innate immunity. PLoS One 2012;7(4):e34177. [PubMed: 22509276]
12. Viappiani S, Nicolescu AC, Holt A, Sawicki G, Crawford BD, Leon H, van Mulligen T, Schulz R. Activation and modulation of 72kDa matrix metalloproteinase-2 by peroxynitrite and glutathione. Biochem Pharmacol 2009;77(5):826–34. [PubMed: 19046943]
13. Ali MA, Cho WJ, Hudson B, Kassiri Z, Granzier H, Schulz R. Titin is a target of matrix metalloproteinase-2: implications in myocardial ischemia/reperfusion injury. Circulation 2010;122(20):2039–47. [PubMed: 21041693]
14. Sawicki G, Leon H, Sawicka J, Sariahmetoglu M, Schulze CJ, Scott PG, Szczesna-Cordary D, Schulz R. Degradation of myosin light chain in isolated rat hearts subjected to ischemia-reperfusion injury: a new intracellular target for matrix metalloproteinase-2. Circulation 2005;112(4):544–52. [PubMed: 16027249]
15. Wang W, Schulze CJ, Suarez-Pinzon WL, Dyck JR, Sawicki G, Schulz R. Intracellular action of matrix metalloproteinase-2 accounts for acute myocardial ischemia and reperfusion injury. Circulation 2002;106(12):1543–9. [PubMed: 12234962]
16. Lovett DH, Chu C, Wang G, Ratcliffe MB, Baker AJ. A N-terminal truncated intracellular isoform of matrix metalloproteinase-2 impairs contractility of mouse myocardium. Front Physiol 2014;5:363. [PubMed: 25309453]
17. Heart Outcomes Prevention Evaluation Study I, Yusuf S, Dagenais G, Pogue J, Bosch J, Sleight P. Vitamin E supplementation and cardiovascular events in high-risk patients. N Engl J Med 2000;342(3):154–60. [PubMed: 10639540]
18. Sawyer DB. Oxidative stress in heart failure: what are we missing? Am J Med Sci 2011;342(2):120–4. [PubMed: 21747279]
19. Reid B, Gibson M, Singh A, Taube J, Furlong C, Murcia M, Elisseeff J. PEG hydrogel degradation and the role of the surrounding tissue environment. J Tissue Eng Regen Med 2015;9(3):315–8. [PubMed: 23495204]
20. Ulbricht J, Jordan R, Luxenhofer R. On the biodegradability of polyethylene glycol, polypeptoids and poly(2-oxazoline)s. Biomaterials 2014;35(17):4848–61. [PubMed: 24651032]
21. Pollock JF, Healy KE. Mechanical and swelling characterization of poly(N-isopropyl acrylamide - co- methoxy poly(ethylene glycol) methacrylate) sol–gels. Acta Biomaterialia 2010;6(4):1307–1318. [PubMed: 19941981]

22. Yang J, van Lith R, Baler K, Hoshi RA, Ameer GA. A thermoresponsive biodegradable polymer with intrinsic antioxidant properties. Biomacromolecules 2014;15(11):3942–52. [PubMed: 25295411]
23. Zhu Y, Matsumura Y, Velayutham M, Foley LM, Hitchens TK, Wagner WR. Reactive oxygen species scavenging with a biodegradable, thermally responsive hydrogel compatible with soft tissue injection. Biomaterials 2018;177:98–112. [PubMed: 29886387]
24. Spaulding K, Takaba K, Collins A, Faraji F, Wang G, Aguayo E, Ge L, Saloner D, Wallace AW, Baker AJ and others. Short term doxycycline treatment induces sustained improvement in myocardial infarction border zone contractility. PLoS One 2018;13(2):e0192720. [PubMed: 29432443]
25. Walker JC, Guccione JM, Jiang Y, Zhang P, Wallace AW, Hsu EW, Ratcliffe MB. Helical myofiber orientation after myocardial infarction and left ventricular surgical restoration in sheep. J Thorac Cardiovasc Surg 2005;129(2):382–90. [PubMed: 15678050]
26. Bashir MR, Bhatti L, Marin D, Nelson RC. Emerging applications for ferumoxytol as a contrast agent in MRI. J Magn Reson Imaging 2015;41(4):884–98. [PubMed: 24974785]
27. Dubois E The estimation of the surface area of the body. In: Dubois E, editor. Basal metabolism in health and disease. Philadelphia, PA: Lea and Febiger; 1936. p 125–144.
28. Gutgesell HP, Rembold CM. Growth of the human heart relative to body surface area. Am J Cardiol 1990;65(9):662–8. [PubMed: 2309636]
29. Wanga S, Ceron CS, Delgado C, Joshi SK, Spaulding K, Walker JP, Song S, Olson JL, Lovett DH. Two Distinct Isoforms of Matrix Metalloproteinase-2 Are Associated with Human Delayed Kidney Graft Function. PLoS One 2015;10(9):e0136276. [PubMed: 26379248]
30. Robinson KM, Janes MS, Pehar M, Monette JS, Ross MF, Hagen TM, Murphy MP, Beckman JS. Selective fluorescent imaging of superoxide in vivo using ethidium-based probes. Proc Natl Acad Sci U S A 2006;103(41):15038–43. [PubMed: 17015830]
31. Kleinbaum DG. Applied regression analysis and other multivariable methods. Belmont: Thomson Brooks/Cole Publishing; 2008.
32. Veterinary Manual. Merck Manual: Merck Sharp & Dohme Corp; 2018.
33. Ifkovits JL, Tous E, Minakawa M, Morita M, Robb JD, Koomalsingh KJ, Gorman JH 3rd, Gorman RC, Burdick JA. Injectable hydrogel properties influence infarct expansion and extent of postinfarction left ventricular remodeling in an ovine model. Proc Natl Acad Sci U S A 2010;107(25):11507–12. [PubMed: 20534527]
34. Zhu Y, Hideyoshi S, Jiang H, Matsumura Y, Dziki JL, LoPresti ST, Huleihel L, Faria GNF, Fuhrman LC, Lodono R and others. Injectable, porous, biohybrid hydrogels incorporating decellularized tissue components for soft tissue applications. Acta Biomaterialia 2018;73:112–126. [PubMed: 29649634]
35. Sun Y. Myocardial repair/remodelling following infarction: roles of local factors. Cardiovasc Res 2009;81(3):482–90. [PubMed: 19050008]
36. Riba A, Deres L, Eros K, Szabo A, Magyar K, Sumegi B, Toth K, Halmosi R, Szabados E. Doxycycline protects against ROS-induced mitochondrial fragmentation and ISO-induced heart failure. PLoS One 2017;12(4):e0175195. [PubMed: 28384228]
37. Rane AA, Chuang JS, Shah A, Hu DP, Dalton ND, Gu Y, Peterson KL, Omens JH, Christman KL. Increased infarct wall thickness by a bio-inert material is insufficient to prevent negative left ventricular remodeling after myocardial infarction. PLoS One 2011;6(6):e21571. [PubMed: 21731777]
38. Morita M, Eckert CE, Matsuzaki K, Noma M, Ryan LP, Burdick JA, Jackson BM, Gorman JH 3rd, Sacks MS, Gorman RC. Modification of infarct material properties limits adverse ventricular remodeling. Ann Thorac Surg 2011;92(2):617–24. [PubMed: 21801916]
39. Sundaram H, Voigts B, Beer K, Meland M. Comparison of the rheological properties of viscosity and elasticity in two categories of soft tissue fillers: calcium hydroxylapatite and hyaluronic acid. Dermatol Surg 2010;36 Suppl 3:1859–65. [PubMed: 20969663]
40. Tous E, Ifkovits JL, Koomalsingh KJ, Shuto T, Soeda T, Kondo N, Gorman JH 3rd, Gorman RC, Burdick JA. Influence of injectable hyaluronic acid hydrogel degradation behavior on infarction-induced ventricular remodeling. Biomacromolecules 2011;12(11):4127–35. [PubMed: 21967486]

41. Kim YK, Kim SJ, Kramer CM, Yatani A, Takagi G, Mankad S, Szigeti GP, Singh D, Bishop SP, Shannon RP and others. Altered excitation-contraction coupling in myocytes from remodeled myocardium after chronic myocardial infarction. J Mol Cell Cardiol 2002;34(1):63–73. [PubMed: 11812165]

42. Hu Q, Wang X, Lee J, Mansoor A, Liu J, Zeng L, Swingen C, Zhang G, Feygin J, Ochiai K and others. Profound bioenergetic abnormalities in peri-infarct myocardial regions. Am J Physiol Heart Circ Physiol 2006;291(2):H648–57. [PubMed: 16582014]

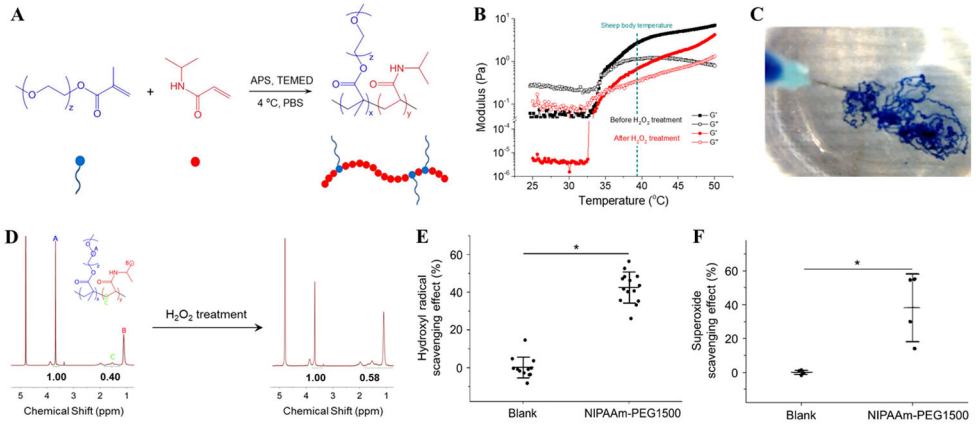

Figure 1.

Poly(NIPAAm-mPEGMA) (NIPAAm-PEG1500) synthesis and characterization. (**A**) Scheme of NIPAAm-PEG1500 synthesis. (**B**) Thermal sensitivity and gelation of NIPAAm-PEG1500 hydrogel (2 wt% in water) before and after H_2O_2 treatment. Both pristine and H_2O_2 treated copolymer gelled at 35°C. G'=storage modulus, G"=loss modulus. (**C**) Injectability of NIPAAm-PEG1500 hydrogel and instant gelation in 37°C water bath. Hydrogel was colored with a blue food dye as a fiduciary marker. (**D**) ^1H nuclear magnetic resonance (NMR) spectrum of NIPAAm-PEG1500 before and after H_2O_2 treatment. (**E**) Inhibition/scavenging effect of NIPAAm-PEG 1500 hydrogel on hydroxyl radical generation characterized by Fenton reaction. (**F**) Scavenging effect of NIPAAm-PEG 1500 hydrogel on superoxide radicals characterized by Pyrogallol assay. * Significant difference, $p < 0.05$.

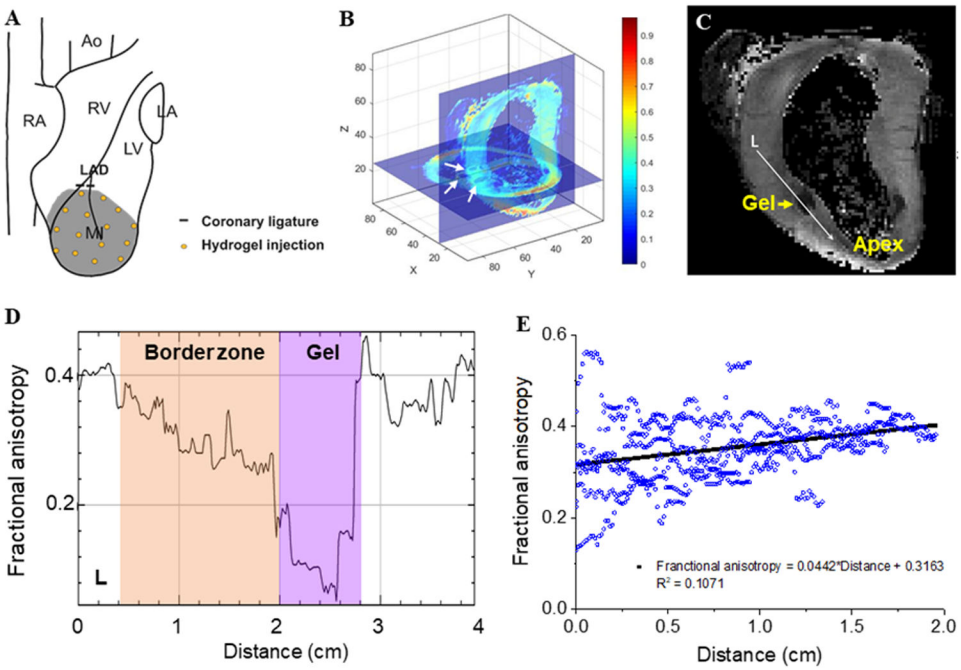

Figure 2.

Pattern of distribution immediately after NIPAAm-PEG1500 hydrogel injection. (**A**) Approximate injection locations. (**B,C**) DT MRI based fractional anisotropy (FA) mapping. (**B**) XY (short axis) and YZ (long axis) slice planes of a representative heart. White arrows: cross sections of hydrogel depot. (**C**) Gray value image of YZ (long axis) slice in (**B**). FA in the longitudinal direction (white arrow (**L**) was measured and plotted in (**D**). Panel (**E**) shows the effect of distance from MI/ BZ border on FA from six depots.

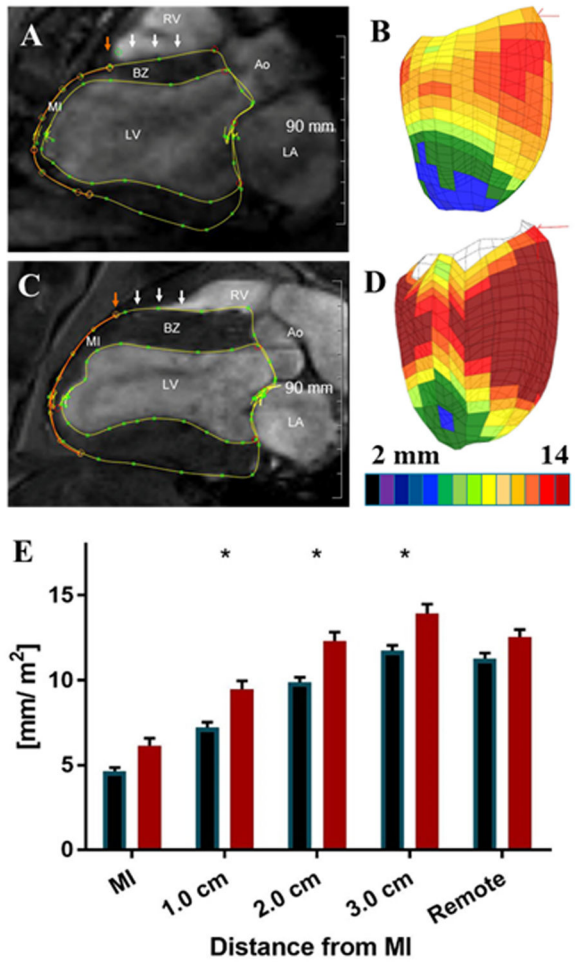

Figure 3.

(**A,B**) *in-vivo* 3T CMRI (long axis) and image based color maps of LV wall thickness at end-systole (ES)6 weeks after MI from representative MI control. (**C,D**) *in-vivo* 3T CMRI (long axis) and image based color maps of LV wall thickness at ES 6 weeks after MI from representative NIPAAm-PEG1500 treated hearts. Epicardial and endocardial contour lines are in yellow. The red circle is the manually determined infarct edge. White arrows mark the points of wall thickness measurement 0.5, 1, 2, and 3 cm from the infarct edge. Color maps are oriented with the anterior wall toward the viewer and colors range from black (< 2 mm) to brown (>14 mm). (**E**) The effect of NIPAAm-PEG1500 hydrogel on LV wall thickness at ES 6 weeks after MI as a function of distance from the MI.

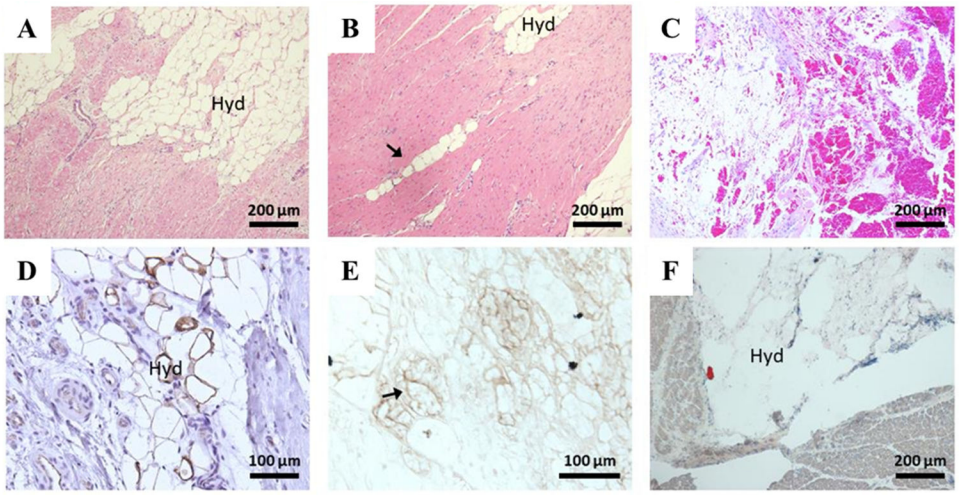

Figure 4.

Histology of NIPAAm-PEG1500 hydrogel at the MI BZ. (**A-C**) samples stained with hematoxylin and eosin. The arrow in (**B**) indicates the migration of the hydrogel into the BZ along planes between myofibers. (**D,E**) are samples immuno-stained with CD31 (**D**) and avidin horse radish peroxidase (**E**). The arrow in (**E**) highlights the outline of positively stained biotin conjugated hydrogel. (**F**) representative staining with oil red O staining, no fat was found. All tissue was paraffin embedded except (**F**), which was frozen section. Hyd=NIPAAm-PEG1500 hydrogel.

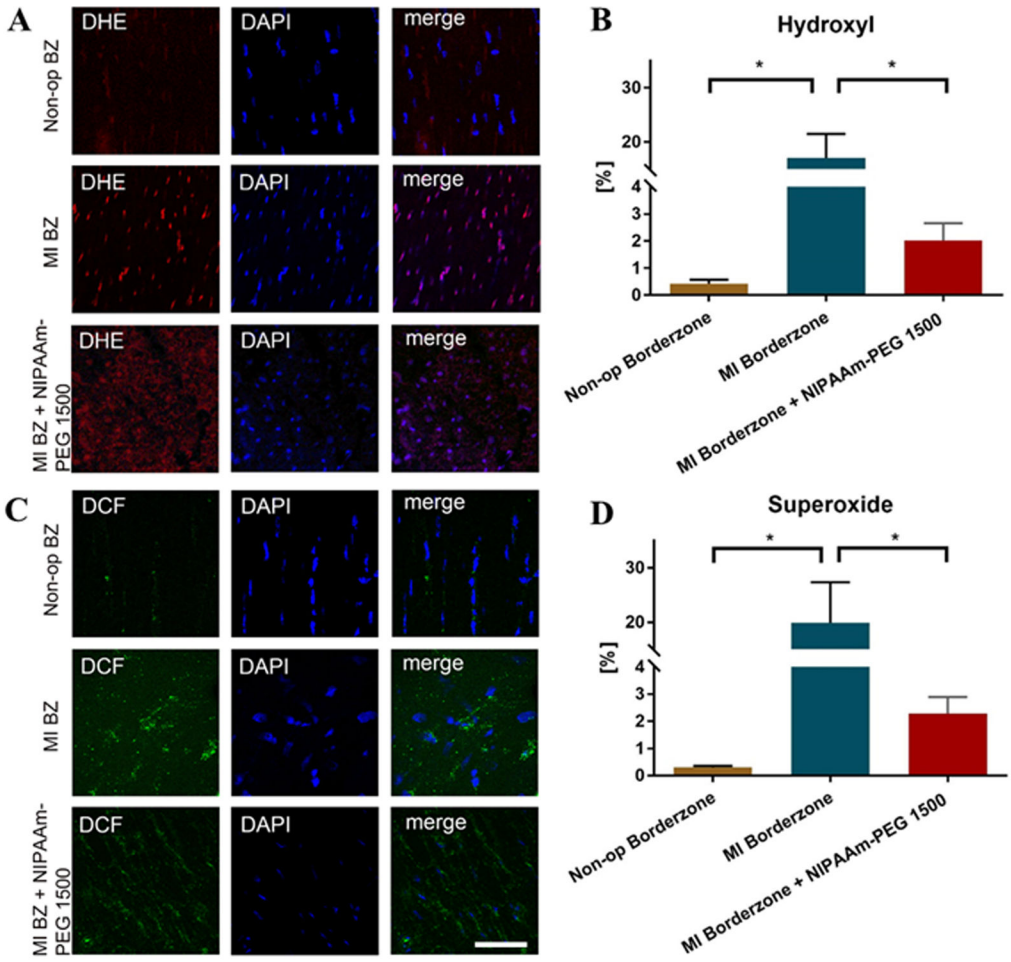

Figure 5.

Effect of NIPAAm-PEG1500 hydrogel on superoxide **(A)** and hydroxide (**B**) 6 weeks after MI. Superoxide was measured with dihydroethidium (DHE) and hydroxide was measured with dichlorfluorescein (DCF). (**C,D**) % area of superoxide (DHE) and hydrogen peroxide (DCF) staining respectively. Scale bar = 50 μm. *Significant difference, $p<0.05$

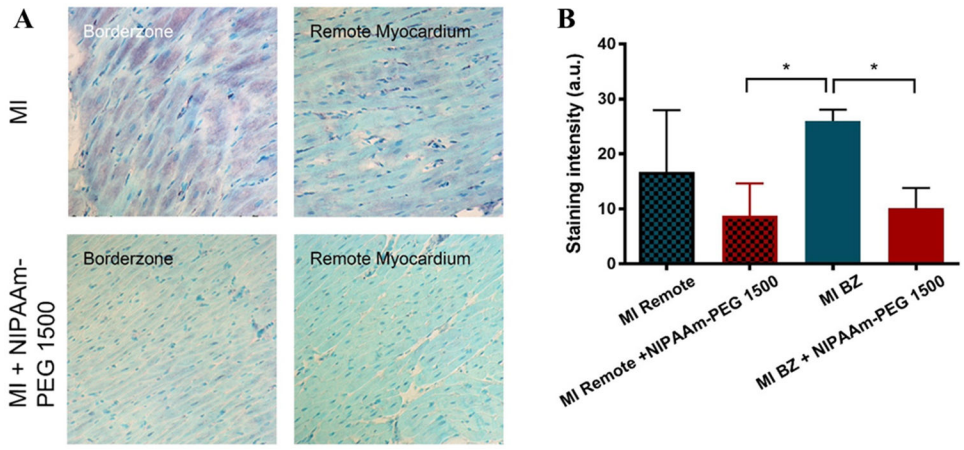

Figure 6.

Effect of NIPAAm-PEG1500 hydrogel on MMP-2 level in the infarct BZ 6 weeks after MI (**A**). (**B**) % area of MMP-2 staining. *Significant difference, $p<0.05$

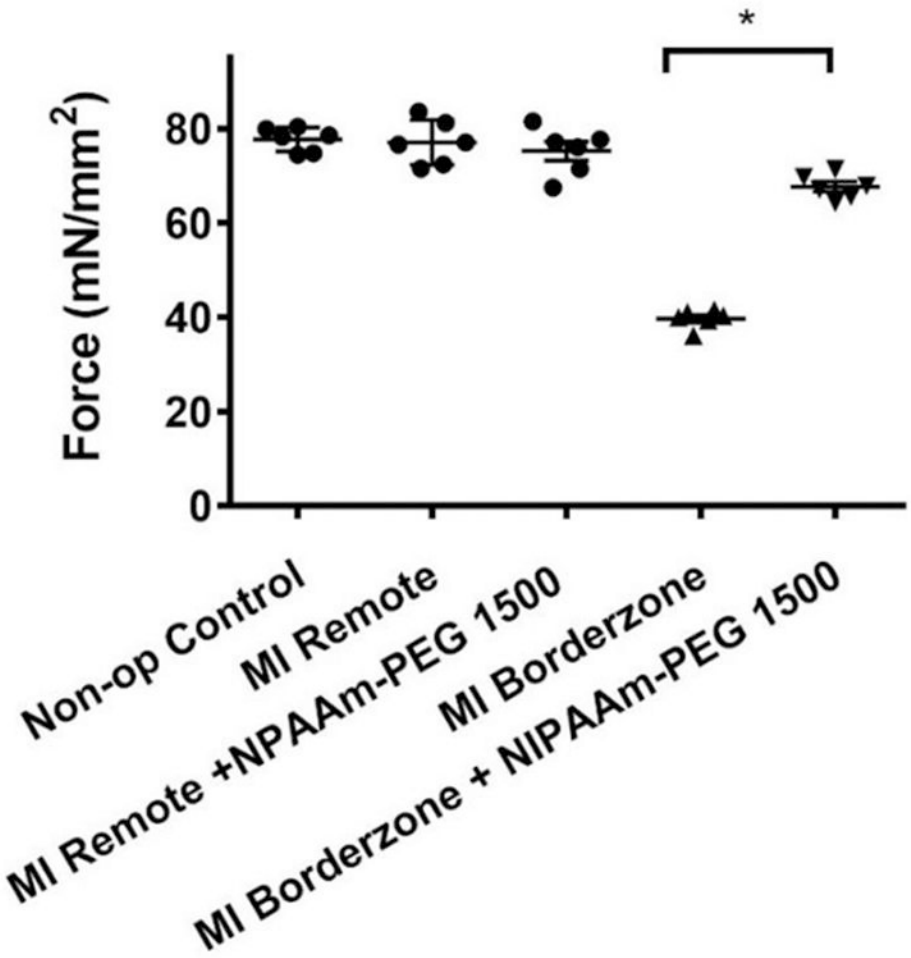

Figure 7.
Effect of NIPAAm-PEG1500 hydrogel on maximum skinned fiber developed force 6 weeks after MI. *Significant difference, $p<0.05$.